JACS JOURNAL OF THE AMERICAN CHEMICAL SOCIETY

Article

pubs.acs.org/JACS

Single-Component Molecular Conductor $[Cu(dmdt)_2]$ with Three-Dimensionally Arranged Magnetic Moments Exhibiting a Coupled Electric and Magnetic Transition

Biao Zhou,[†] Yuki Idobata,[†] Akiko Kobayashi,*[,†] HengBo Cui,[‡] Reizo Kato,[‡] Rina Takagi,[§] Kazuya Miyagawa,[§] Kazushi Kanoda,[§] and Hayao Kobayashi*[,†]

[†]Department of Chemistry, College of Humanities and Sciences, Nihon University, Sakurajosui 3-25-40, Setagaya-Ku, Tokyo 156-8550, Japan

[‡]Condensed Molecular Materials Laboratory, RIKEN, 2-1 Hirosawa, Wako, Saitama 351-0198, Japan

[§]Department of Applied Physics, The University of Tokyo, Hongo 7-3-1, Bunkyo-ku, Tokyo 113-8656, Japan

Supporting Information

ABSTRACT: Crystals of the single-component molecular conductor $[Cu(dmdt)_2]$ (dmdt = dimethyltetrathiafulvalenedithiolate) were prepared as a molecular system, with three-dimensionally arranged magnetic moments embedded in "sea" of π conduction electrons. $[Cu(dmdt)_2]$ had fairly large room-temperature conductivity (110 $S\,cm^{-1}$) and exhibited weakly metallic behavior near room temperature. Below 265 K, the resistivity (R) increased very slowly with decreasing temperature and then increased rapidly, indicating a transition from a highly conducting state to an insulating state near 95 K. The magnetic susceptibility showed Curie–Weiss behavior at 100–300 K (C = 0.375 emu/mol, Θ = 180 K). The Curie constant and the high-temperature resistivity behavior indicate that conduction electrons and three-dimensionally arranged magnetic moments coexist in the crystal. The ESR intensity increased down to about 95 K. The ESR signal was broadened and decreased abruptly near 95 K, suggesting that electric and antiferromagnetic transitions occurred simultaneously near 95 K. The crystal structure was determined down to 13 K. To examine the stability of the twisted conformation of Cu complex with dithiolate ligands, the dihedral angle dependence of the conformational energy of an isolated $M(L)_2^{n-}$ molecule was calculated, which revealed the dihedral angle dependence on the ligand (L) and the oxidation state of the molecule (n). High-pressure four-probe resistivity measurements were performed at 3.3–9.3 GPa using a diamond anvil cell. The small resistivity increase observed at 3.3 GPa below 60 K suggested that the insulating transition observed at ambient pressure near 95 K was essentially suppressed at 3.3 GPa. The intermolecular magnetic interactions were examined on the basis of simple mean field theory of antiferromagnetic transition and the calculated intermolecular overlap integrals of the singly occupied molecular orbital (SOMO) of $Cu(dmdt)_2$.

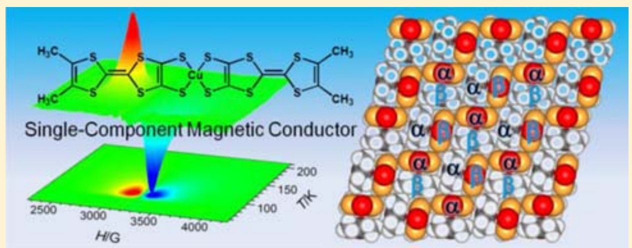

1. INTRODUCTION

Since the discovery of the first single-component molecular metal, $[Ni(tmdt)_2]$ (tmdt = trimethylenetetrathiafulvalenedithiolate), with a stable metallic state down to 0.6 K, a series of isostructural systems, $[M(tmdt)_2]$ (M = Ni, Pd, Pt, Au, Cu) have been developed.[1−3] In the crystal, the planar $M(tmdt)_2$ molecules are closely packed to form layers parallel to the molecular plane, and these layers are stacked closely to produce three-dimensional metal bands formed from π -like frontier orbitals. $[M(tmdt)_2]$ exhibits a variety of electronic properties upon exchange of the central metal atom (M) for other transition metals. For example, $[Au(tmdt)_2]$ undergoes an antiferromagnetic transition at 110 K while retaining its metallic state down to low temperature.[4] The three-dimensionality of the electronic band structure characteristic of $[M(tmdt)_2]$ is considered to be the origin of the very high magnetic transition temperature of $[Au(tmdt)_2]$ relative to those of traditional molecular conductors.[5,6] Unlike $[M(tmdt)_2]$ (M = Ni, Au),[4,7] the energy level of the d-like orbital of $Cu(tmdt)_2$ (or the $pd\sigma(-)$ orbital), with large amplitude at the $\{CuS_4\}$ center, is approximately equal to the energy level of the π-like frontier orbitals (or conduction molecular orbitals) delocalized over the whole molecule. This is unprecedented among molecular conductors, which makes the electromagnetic properties of the Cu-containing single-component molecular conductor very attractive. It was reported that the one-dimensional Heisenberg chain originated from the intermolecular overlap of the $pd\sigma(-)$ orbitals and π-like conduction bands coexisted in $[Cu(tmdt)_2]$.[8] On the other hand, the crystal structure of $[Cu(dmdt)_2]$ (dmdt = dimethyltetrathiafulvalenedithiolate) was reported to consist of twisted $Cu(dmdt)_2$ molecules with distorted D_2 symmetry.[9] Since the d orbitals in $Cu(dmdt)_2$ could be easily mixed with ligand π orbitals due to the twisted conformation, the

Received: May 8, 2012
Published: July 3, 2012

electromagnetic properties were expected to be quite different from those of [Cu(tmdt)$_2$]. We previously reported the crystal structure of [Cu(dmdt)$_2$].[9] The physical properties, determined using powder samples (and a poor quality crystal), showed semiconducting behavior (σ(RT) $\approx$ 3 S cm^{-1}) and the existence of 84% of a S = $^1/_2$ localized magnetic moment.[9] The first-principle band structure calculations by Ishibashi et al. suggested an antiferromagnetic ground state for [Cu(dmdt)$_2$].[10] However, no sign of magnetic transition has been observed. Furthermore, our recent synchrotron radiation powder X-ray diffraction experiments at SPring-8 revealed that powder samples of [Cu(dmdt)$_2$] contained more than two polymorphs.

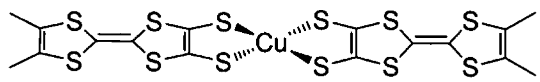

Cu(dmdt)$_2$

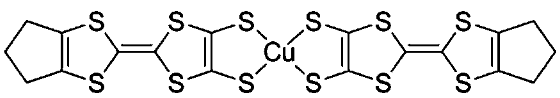

Cu(tmdt)$_2$

We recently tried to grow single crystals of [Cu(dmdt)$_2$] of sufficient quality for analysis. We report herein the results of crystal structure determinations down to 13 K, the temperature dependence of single-crystal resistivity at ambient pressure and at high pressure (up to about 9 GPa), the magnetic phase transition observed near 95 K, and the examination of the stable conformation of the Cu-dithiolate ligand complex. A discussion of the magnetic properties of [Cu(dmdt)$_2$] based on the mean-field theory of antiferromagnetic transition and the results of molecular orbital calculations are also presented.

2. EXPERIMENTAL SECTION

2.1. General Methods. All reactions shown in Scheme 1 were performed under strictly inert atmosphere using Schlenk techniques, because the anionic states of the metal complexes were quite sensitive to oxygen. The dmdt ligand was synthesized by a pseudo-Wittig reaction according to a procedure described in the literature.[11] Copper(II) chloride dihydrate ($Cu^{II}Cl_2{\cdot}2H_2O$) was recrystallized from distilled water and dried in air, and $(Me_4N)_2[CuCl_4]$ was synthesized from $Cu^{II}Cl_2{\cdot}2H_2O$ in ethanol by adding $Me_4N{\cdot}Cl$. Tetrahydrofuran (THF) was freshly distilled under argon atmosphere over sodium and benzophenone. Methanol (MeOH) was distilled under argon atmosphere over magnesium metal activated with iodine. The supporting electrolyte, tetra-*n*-butylammonium hexafluorophosphate ($^nBu_4N{\cdot}PF_6$), used in the electrocrystallization, was recrystallized three times from ethyl acetate and dried *in vacuo*. Acetonitrile (MeCN) was distilled under argon atmosphere in the presence of calcium hydride. All other reagents were used without further purification. In the revised synthesis, purified $(Me_4N)_2[CuCl_4]$ was used in exchange for $Cu^{II}Cl_2{\cdot}2H_2O$ as a copper source, and MeCN was used as the organic solvent for electrocrystallization in exchange for THF.

2.2. Synthesis of $(Me_4N)_2$[Cu(dmdt)$_2$]. In dry THF (10.0 mL), the dmdt ligand (121.0 mg, 0.300 mmol) was dissolved and the solution was hydrolyzed with a 25 wt % MeOH solution of tetramethylammonium hydroxide ($Me_4N{\cdot}OH$) (510 mg, 1.4 mmol) at room temperature under argon atmosphere. The solution was stirred for 30 min, and the color of the solution changed from orange to purple. After cooling to −78 °C in a dry ice/MeOH bath, a solution of $(Me_4N)_2[CuCl_4]$ (55.8 mg, 0.158 mmol) in dry MeOH (5.0 mL) was added dropwise to the reaction mixture. Then the reaction mixture was warmed to room temperature overnight. The resulting microcrystals were collected by filtration to afford dark-orange crystals of $(Me_4N)_2$[Cu(dmdt)$_2$].

Scheme 1

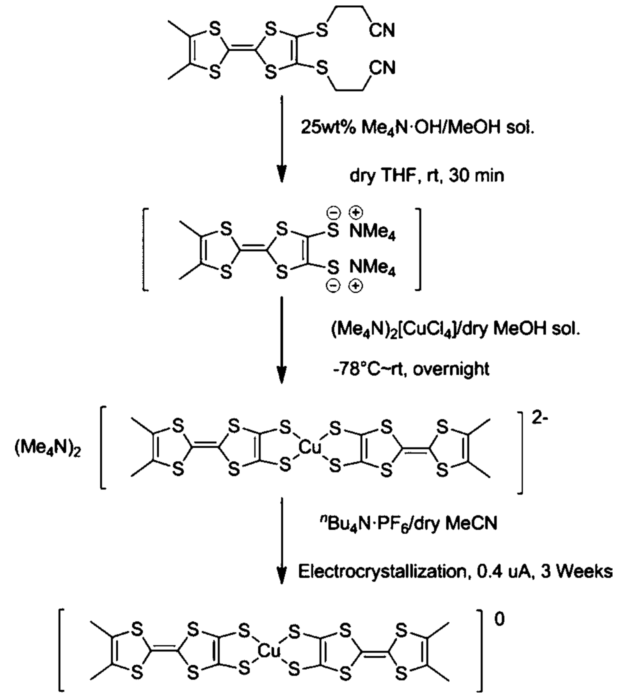

2.3. Electrochemical Synthesis of [Cu(dmdt)$_2$]. Electrochemical oxidations were performed in a standard H-type cell without glass frits using two platinum electrodes under argon atmosphere. $(Me_4N)_2$[Cu(dmdt)$_2$] (10 mg, 0.012 mmol) and $^nBu_4N{\cdot}PF_6$ (120.0 mg, 0.31 mmol) as the electrolyte were dissolved in dry MeCN (20.0 mL) under argon atmosphere. Electrochemical oxidation of this solution was performed with a constant current of 0.4 μA at room temperature. Air-stable black crystals of [Cu(dmdt)$_2$] grew on the Pt electrode within approximately 3 weeks.

2.4. Crystal Structure Determination of [Cu(dmdt)$_2$]. Single-crystal X-ray structure determinations were carried out at 293 K, 250 K, 200 K, 180 K, 150 K, 120 K, 90 K, 65 K, 40 K, and 13 K. The X-ray intensity measurements were carried out on a Rigaku Micro7HFM-VariMax Saturn 724R CCD system equipped with graphite-monochromated Mo Kα radiation (λ = 0.7107 Å) and a confocal X-ray mirror. The crystal data are presented in the Supporting Information (Table S1). The crystal structures were refined with anisotropic temperature factors for non-hydrogen atoms. The calculated positions of the hydrogen atoms were not refined but were included in the final calculations. All calculations were performed using the Crystal Structure crystallographic software package of the Molecular Structure Corp.[12]

2.5. Electrical Resistivity Measurements of [Cu(dmdt)$_2$] at Ambient Pressure. Four-probe resistance measurements were performed in the temperature range of 9−300 K using single crystals with a maximum size of approximately 0.35 mm. Annealed gold wires (10 μm in diameter) bonded to the sample by a mixture of gold and carbon paint were used as leads.

2.6. Magnetic Measurements. Magnetic measurements were performed with a Quantum Design MPMS-7XL superconducting quantum interference device (SQUID) magnetometer in the temperature range from 2.0 to 300 K at an applied magnetic field of 0.5 T. To avoid contamination from different polymorphic crystals, X-ray examinations were performed on many single crystals. This confirmed that crystals with the same morphology were the same polymorph. A polycrystalline sample (1.28 mg, 1.96 × 10^{-3} mmol) of [Cu(dmdt)$_2$] was used because it was not easy to collect a larger amount of isomorphic single crystals of [Cu(dmdt)$_2$]. The selected samples were wrapped in clean aluminum foil (for which magnetic susceptibility was separately measured and subtracted). The diamagnetic contribution (−3.15 × 10^{-4} emu/mol) was estimated from Pascal's constants.

 dx.doi.org/10.1021/ja3044757 | J. Am. Chem. Soc. 2012, 134, 12724−12731

2.7. Electron Spin Resonance (ESR) Measurements. The ESR spectra of [Cu(dmdt)$_2$] were measured over the temperature range 2.5−293 K using polycrystalline samples. Isomorphic single crystals of [Cu(dmdt)$_2$] (0.4 mg, 0.6 × 10^{-3} mmol) were gathered. A JEOL JES-FA300 ESR spectrometer and a low-temperature unit (JEOL ES-CT470) were used. The applied microwave power was 1.0 mW and the modulation field was about 20 G.

2.8. Molecular Orbital Calculations. Spin-polarized and non-spin-polarized calculations were performed at the density functional theory (DFT) level with DMol^3 codes[13,14] using the Generalized Gradient Approximation (GGA) and the exchange and correlation functionals of Becke−Lee−Yang−Parr (BLYP), respectively. Double numerical basis sets plus polarization functions (DNP) were used in the calculations with a global orbital cutoff of 4.4 Å. The density convergence criterion for the self-consistent field optimization energy was set to 10^{-6} hartree. With the aim of a qualitative estimation of the intermolecular magnetic interactions, the intermolecular overlap integrals of the singly occupied molecular orbital (SOMO) of [Cu(dmdt)$_2$] were also calculated on the basis of extended Hückel approximations.

2.9. High Pressure Resistivity Measurements using a Diamond Anvil Cell (DAC). About 15 years ago, we tried to measure the resistivity of [Ni(ptdt)$_2$] up to 7 GPa using a diamond anvil cell (DAC).[15] More recently, we succeeded in realizing the pressure-induced metallization of [Ni(ptdt)$_2$] at very high pressure (∼19 GPa) by adopting a newly improved technique for DAC four-probe resistivity measurements.[16] In the present experiments, we used the epoxy encapsulation method to reduce uniaxial effects.

After four 5 μm gold wires were attached to the sample crystal, the crystal was encapsulated in a thin layer of alumina-reinforced epoxy. Since the inner diameter of the gasket shrinks with pressure, the sample space was limited to less than 0.15 mm. A crystal with dimensions of 0.11 (length) × 0.04 (width) × 0.01 (thickness) mm^3 was used. The Stainless Steel 301 was used as the metal gasket. A hard stainless steel needle was used to make approximately 20 μm wide by 20 μm deep grooves in the gasket, which were then filled with a mixture of alumina and epoxy resin. Then the sample crystal was placed in the sample chamber of the DAC. Daphne Oil 7373 was used as the pressure medium. The pressure was determined at room temperature by monitoring the shift of the ruby fluorescence R_1 line.

3. RESULTS AND DISCUSSION

3.1. Electrical Properties of [Cu(dmdt)$_2$] at Ambient Pressure. The temperature dependence of the electrical resistivity of [Cu(dmdt)$_2$] is shown in Figure 1. The room-temperature conductivity was 110 S cm^{-1}, which was about 30 times higher than the reported conductivity of the compressed pellet of the powder sample.[9] The temperature dependence was weakly metallic around room temperature. Between 270−150 K, the resistivity (R) was approximately constant, and then increased very slowly with decreasing temperature (R(150 K)/R(270 K) ≈ 2.0. Below 100 K, R increased rapidly. (dln$R$/dT) showed a maximum near 90 K (see the inset (left) of Figure 1), indicating the transition from a highly conducting state to an insulating state.

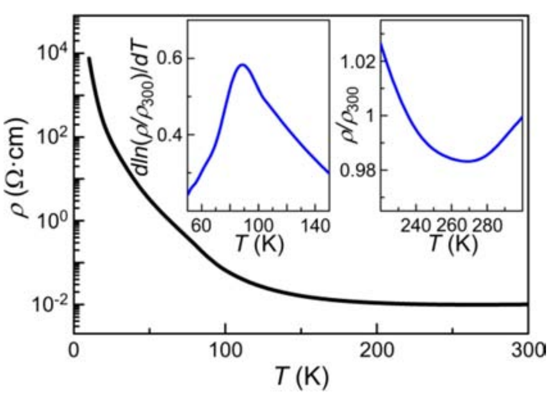

Figure 1. Temperature dependence of electrical resistivity in [Cu(dmdt)$_2$]. The insets indicate weakly metallic behavior near room temperature and the existence of an electric transition near 90 K.

3.2. Magnetic Properties of [Cu(dmdt)$_2$]. At low temperatures, the susceptibility obtained using a SQUID magnetometer increased with decreasing temperature (Figure 2a), which was attributed to the 2.5% paramagnetic impurities

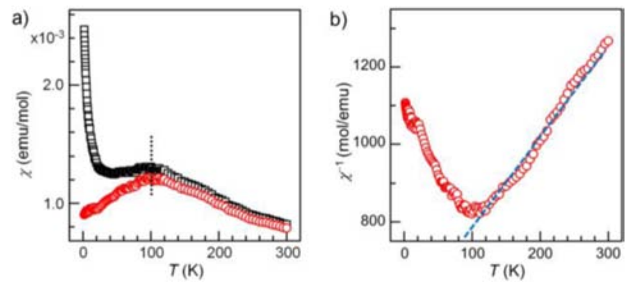

Figure 2. (a) Temperature dependence of magnetic susceptibility (χ) in [Cu(dmdt)$_2$]. The red circles show magnetic susceptibility subtracted 2.5% impurity. (b) χ^{-1} vs T plot showing the magnetic phase transition near 95 K.

with $S = {}^1/_2$ moments. Due to the large impurity peak, accurate low-temperature magnetic behavior was hardly detected. In contrast to the fairly high conductivity and weakly metallic behavior near room temperature, the susceptibility behavior was far from simple Pauli-like. The susceptibility increased with decreasing temperature and showed a peak near 100 K. We previously reported one-dimensional Heisenberg behavior in [Cu(tmdt)$_2$], where the antiferromagnetic interaction was considered to originate from the intermolecular overlap of $dp\sigma(-)$ orbitals along the a direction.[8] However, the molecular arrangement in [Cu(dmdt)$_2$] was completely different from that of [Cu(tmdt)$_2$].[8,9] Unexpectedly, between 100−300 K, the magnetic susceptibility showed Curie−Weiss behavior: $\chi = C/(T + 180)$ (Figure 2). The Curie constant C (= 0.375 emu/mol) suggested that every Cu(dmdt)$_2$ molecule possessed a magnetic moment of ${}^1/_2$ spin ($g \approx 2.0$). The Weiss temperature of −180 K indicated a fairly strong intermolecular antiferromagnetic interaction. The magnetic susceptibility showed a broad peak near 95 K (Figure 2). These behaviors suggested an antiferromagnetic nature below about 100 K. The field dependence of the susceptibilities at 0.5−5 T indicated spin-flop-like behavior (see Supporting Information (Figure S2b)), but due to the limited accuracy of the experimental data and the large quantity of low-temperature paramagnetic impurities, the clear field dependence of the susceptibility was not determined.

3.3. Electron Spin Resonance of [Cu(dmdt)$_2$]. ESR spectra of polycrystalline [Cu(dmdt)$_2$] samples were measured between 2.5−293 K (Figure 3). The temperature dependence of the ESR intensity is shown in Figure 3a. The peak-to-peak linewidths (ΔH_{pp}) and g values are shown in Figure 3c. Around 180 K, the peak-to-peak line width was more than 800 G, and at 97 K, the line width decreased to 180 G. The g value was 2.025 around 180 K and decreased slightly with decreasing temperature down to 97 K, where the g value was 2.018. The spin susceptibility (χ_s) at 97 K was 1.4 × 10^{-3} emu/mol, which was in good agreement with the above-mentioned magnetic

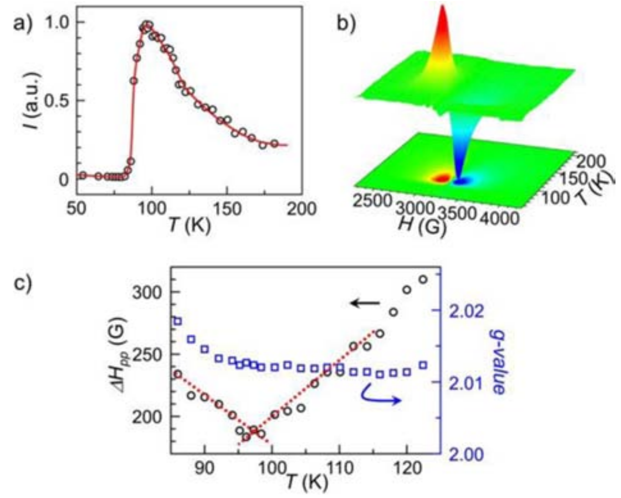

Figure 3. (a) Temperature dependence of the spin susceptibility of [$Cu(dmdt)_2$]. (b) Three-dimensional spectra of ESR of [$Cu(dmdt)_2$]. (c) Temperature dependence of the peak-to-peak line width and g-value of [$Cu(dmdt)_2$].

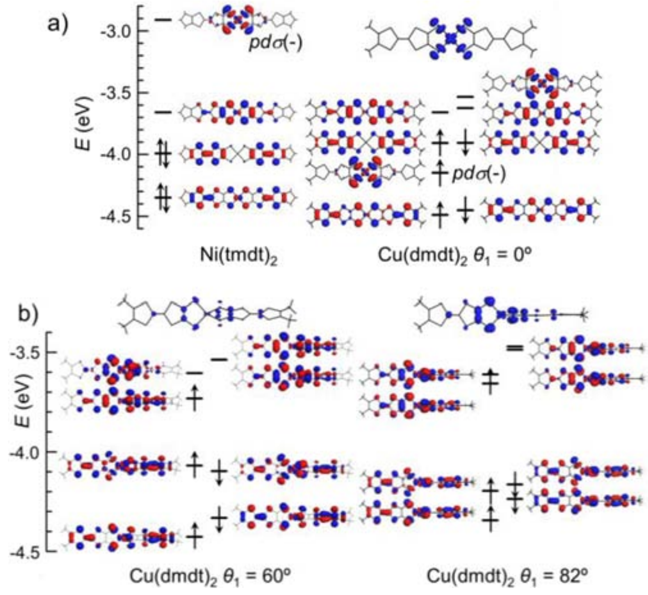

Figure 4. (a) Nonspin-polarized MOs of $Ni(tmdt)_2$ and spin-polarized MOs of the planar $Cu(dmdt)_2$ molecule, where θ_1 is the dihedral angle between two dmdt ligands. The calculated spin density of $Cu(dmdt)_2$ is also presented. (b) Spin-polarized MOs and spin density of twisted $Cu(dmdt)_2$ molecule (θ_1 = 60°, 82°).

susceptibility (χ) obtained by SQUID (1.3×10^{-3} emu/mol at 97 K). The ESR intensity increased down to 100 K and then decreased abruptly near 97 K, where the onset of an increase in line width was observed. Below 80 K, there remained a signal smaller than 1% of the maximum peak at 97 K, which was ascribable to paramagnetic impurities. The ESR observations, the fairly large antiferromagnetic interaction between the three-dimensionally arranged magnetic moments suggested by the Curie−Weiss behavior of the susceptibility, and the temperature dependence of the resistivity, indicated that [$Cu(dmdt)_2$] undergoes a coupled electric and antiferromagnetic transition near 95 K.

More than a quarter century ago, Hunig et al. reported remarkable Cu-containing organic conductors (R_1,R_2-DCNQI)$_2$Cu (R_1, R_2 = Me, Cl, Br) that exhibited a variety of electromagnetic properties, which aroused a considerable interest around those days.[17,18] Since then, the development of novel magnetic molecular conductors has become one of the main targets in the chemistry of molecular conductors. However, in the case of (R_1,R_2-DCNQI)$_2$Cu systems, the interaction between magnetic moments and π metal electrons could not be realized because the magnetic moments of Cu^{2+} ions were found to appear only in the insulating state. More than a decade ago, various remarkable magnetic organic metals and superconductors, consisting of conduction layers of organic π-donor molecules (D) and magnetic anions (X), were discovered.[19,20] However, it is very hard to develop the D_2X type conductor with sufficiently large interactions between magnetic moments and conduction electrons because the conduction electrons and localized magnetic moments are spatially separated in these systems. In contrast, the single component molecular conductors, [$Cu(L)_2$], are considered to be very suitable systems for developing new molecular conductors that exhibit unprecedentedly large interactions between conduction electrons and localized magnetic moments.

As shown in Figure 4, the calculated molecular orbitals and spin densities of $Cu(L)_2$ (L = dmdt, tmdt) suggested that the unpaired spins are distributed mainly in the SOMO. In contrast to $Cu(tmdt)_2$ with a σ−type SOMO (or $pd\sigma(-)$ orbital) distributed in the central {CuS_4} part of the molecule,[10] $Cu(dmdt)_2$ with its twisted structure has much wider spin distribution due to mixing between the π (ligand) and d (Cu) orbitals. Consequently, a larger interaction will be expected between conduction electrons and localized magnetic moments in [$Cu(dmdt)_2$], where the conduction band is formed mainly by intermolecular overlap of ligand orbitals. The coexistence of the fairly large conductivity (110 S cm^{-1} at 293 K) and the three-dimensionally arranged spin $^1/_2$ moments embedded in the "sea of π conduction electrons" cannot be realized in the D_2X-type traditional molecular conductors. We recently reported a molecular alloy with diluted magnetic moments (or a molecular Kondo system), [$Ni_{1-x}Cu_x(tmdt)_2$ (x < 0.2)].[21] On the other hand, [$Cu(dmdt)_2$] seems to provide a cue toward realizing an unprecedented "molecular dense-Kondo system" where magnetic moments interacting with conduction electrons are arranged three-dimensionally.

3.4. X-ray Structural Studies at Low Temperatures. To increase our understanding of the physical properties of [$Cu(dmdt)_2$], single crystal X-ray structure determinations were carried out at 10 different temperatures between 13 and 293 K (Table S1, Supporting Information). Due to the improved crystal quality, the standard deviations of molecular dimensions could be much reduced compared with those from the previously determined room-temperature structure of [$Cu(dmdt)_2$].[9] The temperature dependence of the lattice constants is shown in Figure 5a (and Figure S1, Supporting Information). The crystal structures were almost unchanged down to 13 K. That is, the electric and magnetic transitions observed near 95 K were not accompanied by a distinct structural change. The crystal structure and the mode of molecular packing at 13 K are shown in Figures 5b and 6a. As reported,[9] the unit cell contains four $Cu(dmdt)_2$ molecules and all the molecules are crystallographically equivalent. The central Cu atom has a tetrahedral geometry and $Cu(dmdt)_2$ has a twisted molecular structure. The average thermal expansion

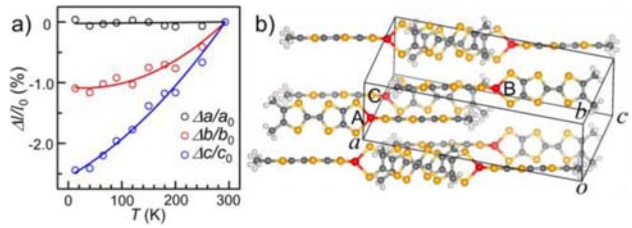

Figure 5. (a) The temperature dependence of the rates of the lattice constants, a, b, and c, of [Cu(dmdt)$_2$]. a_0 (24.921 Å), b_0 (8.254 Å), c_0 (11.529 Å), and l_0 are the lattice constants at 293 K and $\Delta a = a - a_0$, $\Delta b = b - b_0$, and $\Delta c = c - c_0$. The crystal structure of [Cu(dmdt)$_2$] at 13 K. Red, orange, gray, and white spheres represent Cu, S, C, and H atoms, respectively. (b) Molecular arrangement in the [Cu(dmdt)$_2$] crystal viewed along the perpendicular direction of one of the ligand planes.

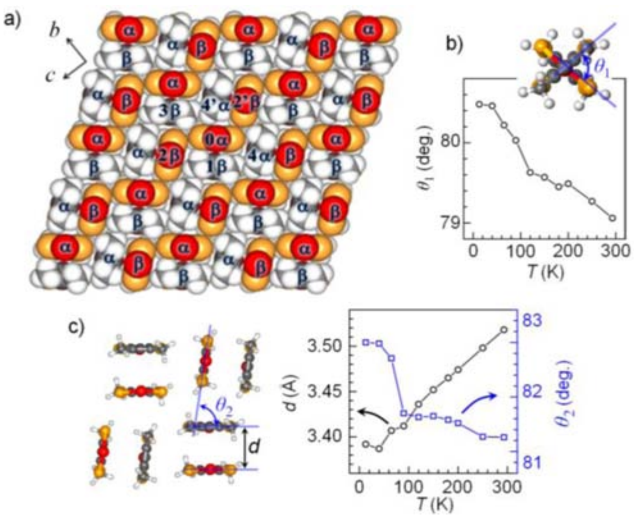

Figure 6. (a) End-on projection of the "κ-type molecular arrangement" and a spin structure model of [Cu(dmdt)$_2$]. α and β denote the molecules with up (α) and down (β) spins, respectively. The numbers 0−4 represent the central Cu(dmdt)$_2$ molecule (0) and surrounding molecules (1−4). (b) The temperature dependence of the twist angle (θ_1) of Cu(dmdt)$_2$. (c) The temperature dependence of the dihedral angle (θ_2) of two dimeric ligands and the intermolecular distance between the dimeric ligands.

coefficients at 100−250 K were $|(\Delta a/\Delta T)/a| < 1 \times 10^{-5}$ K^{-1}, $|(\Delta b/\Delta T)/b| \approx 3.8 \times 10^{-5}$, $|(\Delta c/\Delta T)/c| \approx 8.1 \times 10^{-5}$. Usually, the thermal expansion coefficient of a molecular crystal is much larger than that of an inorganic crystal. However, the thermal expansion coefficient of [Cu(dmdt)$_2$] was found to be essentially zero along the a axis within the accuracy of the experiments over the temperature range 13−250 K (see Figure 5a). It is well-known that the thermal expansion coefficient (α) is roughly proportional to compressibility (κ): $\alpha \approx \gamma\,(C_V\kappa)/V$ (γ = Gruneisen constant). Consequently, the crystal lattice of [Cu(dmdt)$_2$] is considered to be unusually stiff along the a axis. As shown in Figure 5b, the dmdt ligand on the right side of one Cu(dmdt)$_2$ molecule is stacked face-to-face with the ligand on the left side of the neighboring Cu(dmdt)$_2$ molecule to form a "dmdt dimer." "Dmdt dimers" with two different orientations are arranged to form a "dmdt layer" parallel to the bc plane, with an arrangement closely resembling the two-dimensional molecular arrangement in the well-known "κ-type organic superconductors"[22] (Figures 5b and 6a). Furthermore, these "κ-type dmdt layers" are tightly connected to each other by Cu atoms through Cu−S coordination bonds to make the crystal lattice anomalously stiff along the a axis.

The Cu−S bond length (r_{Cu-S}) was slightly decreased with temperature but no significant anomaly could be observed near the transition temperature (∼95 K). It was reported that the r_{Au-S} of the planar Au(tmdt)$_2$ molecule was abruptly shortened (by about 0.007 Å) at the antiferromagnetic transition temperature (T_N = 110 K),[23] below which the development of "intramolecular antiferromagnetic spin structure" was proposed by theoretical calculation.[7] Except for this anomaly, the r_{Au-S} of the Au(tmdt)$_2$ molecule increased with decreasing temperature (r_{Au-S}= 2.308 Å at 300 K and 2.322 Å at 120 K).[23] The origin of the reverse temperature dependence of the Cu−S bond length in Cu(dmdt)$_2$ is not clear at present. The dihedral angle of the two dmdt ligands of Cu(dmdt)$_2$ (θ_1) tended to increase with decreasing temperature but the dihedral angles of the ligands of the neighboring dmdt dimers showed a distinct increase near 90 K (Figures 6b and 6c). There were some intermolecular S···S close contacts shorter than the van der Waals distance (r_{vdW}(S···S) = 3.70 Å) between molecule A (x, y, z) and molecule B ($1/2 - x$, $1/2 - y$, $-z$) (3.695 Å, 3.652 Å), and molecule A (x, y, z) and molecule C ($-x$, $-y$, $-z$) (3.696 Å, 3.455 Å) (see Figure 5b). The S−Cu−S angle was larger than that of the planar [Cu(tmdt)$_2$] molecule (90.9°). The C=C bond length in the five-membered ring CuSCCS (c) was 1.444(3) Å at 293 K, which was much longer than the corresponding C=C bond length of planar [Cu(tmdt)$_2$] (1.379 Å). This is, of course, due to the tetrahedral coordination of Cu(dmdt)$_2$. On the other hand, the other C=C bond lengths were about 1.365 Å (at 293 K), approximately equal to the C=C bonds of Cu(tmdt)$_2$ (∼1.364 Å).

3.5. Stable Conformation of [M(L)$_2$] (L = dithiolate ligand). As mentioned before, Cu(dmdt)$_2$ has a twisted structure in the crystal of [Cu(dmdt)$_2$]. The energies of isolated M(L)$_2$ (M = Ni, Cu, Zn, Au; L = tmdt or dmdt) molecules were calculated as a function of the dihedral angle (θ_1) by Ishibashi (see Figure 6b).[10] The energy minimum was found at 0° for Ni(tmdt)$_2$ and Au(tmdt)$_2$ but was at 82° for Cu(dmdt)$_2$ and at 90° for Zn(tmdt)$_2$. These results were in good agreement with the molecular structures determined by X-ray structure analyses.[9,23,24] However, Cu(tmdt)$_2$ adopted a planar structure in the crystalline state,[8] though the calculated structure of isolated Cu(tmdt)$_2$ was most stable when the molecule had a distorted tetrahedral conformation ($\theta_1 \approx 82°$). The discrepancy between the observed and calculated molecular structures of Cu(tmdt)$_2$ is considered to be due to the small energy difference between the planar and tetrahedral structures and the molecular packing effect in the crystal, because planar M(tmdt)$_2$ molecules with terminal trimethylene groups are closely packed two-dimensionally to produce a compact sheet structure. In contrast, M(dmdt)$_2$ molecules with terminal methyl groups cannot be packed in the same sheet structure. In order to check the stability of the twisted conformation, the θ_1-dependence of the conformation energies of isolated neutral dithiolate complexes, M(L)$_2{}^n$ (M = Cu, Zn; n = 0; L = dmit, ptdt, and dmdt) (ptdt = propylenedithiotetrathiafulvalenedithiolate) were also performed (Figure 7). For comparison, the calculations were also carried out on mono- and dianionic Cu complexes (n = −1, −2), where the monoionic Cu complex has the same total number of electrons as the corresponding neutral Zn complex. The "π-like orbital (p_x or p_y-like orbital)" of M(L)$_2$ with D_{2d} symmetry is doubly

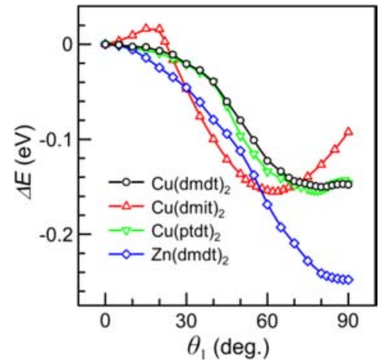

Figure 7. The conformational energy of a neutral $M(L)_2$ (M = Cu, Zn, L = dmdt, dmit, ptdt) molecule as a function of the dihedral angle (θ_1) of two dithiolate ligands (see Figure 6b).

degenerated. Consequently, in contrast to $Zn(L)_2$ with fully occupied d-orbitals, $Cu(L)_2$ with an odd number of total electrons, tends to undergo Jahn−Teller distortion.[7,10] As expected, all neutral Zn complexes were confirmed to exhibit D_{2d} symmetry (θ_1 = 90°) and the neutral $Cu(L)_2$ (L = dmdt, ptdt, n = 0) molecules had slightly distorted tetrahedral conformations ($\theta_1 \approx 82°$). $Cu(L)_2^-$ (L = dmdt, ptdt; $n = -1$) complexes with the same total number of electrons as neutral $Zn(L)_2$ showed an energy minimum at $\theta_1 \approx 75°$. On the other hand, $Cu(dmit)_2^n$ showed an energy minimum at $\theta_1 \approx 65°$, irrespective of the oxidation state (n = 0, −1, −2). This twisted angle of $Cu(dmit)_2^{2-}$ was consistent with the observed molecular conformation in [N-ethylpyridinium][$Cu(dmit)_2$]$_2$ (θ_1 = 65°).[25] It was found that, unlike the neutral Zn complex with D_{2d} symmetry, the calculated stable conformations of isolated mono- and di-ionic Cu-dithiolate complexes did not have D_{2d} conformations. In particular, [$Cu(dmit)_2$] tended to adopt a stable conformation at $\theta_1 \approx 65°$.

3.6. Resistivity Behavior of [Cu(dmdt)$_2$] at High Pressure.

The DAC four-probe resistivity measurements were performed on [$Cu(dmdt)_2$] at 3.3−9.3 GPa (Figure 8). The insulating transition observed near 90 K at ambient pressure was almost suppressed at 3.3 GPa. The resistivity near 10 K was about 10^4 Ω cm at ambient pressure but decreased to about 4×10^{-3} Ω cm at 3.3 GPa. Considering the extremely small increase of the resistivity below 60 K, (R(1.9 K)/R(60 K) ≈ 1.6 at 3.3 GPa, the resistivity increase at low temperature

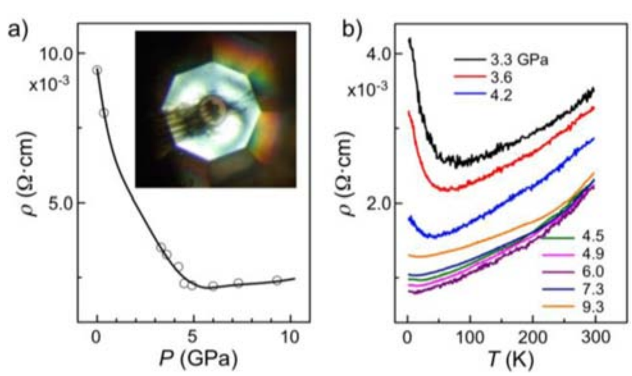

Figure 8. (a) Pressure dependence of the room-temperature resistivity of [$Cu(tmdt)_2$]. (Inset) Sample assembled in a DAC. The resistivity at 3 kbar was obtained using a conventional clamp-type cell. (b) Temperature dependence of the resistance of [$Cu(dmdt)_2$] at 3.3−9.3 GPa.

cannot be considered to reflect the intrinsic semiconducting properties of [$Cu(dmdt)_2$]. Presumably, a high quality crystal of [$Cu(dmdt)_2$] will retain metallic behavior down to low temperature at 3.3 GPa. The suppression of the resistivity increase at low temperatures with increasing pressure (3.3−4.9 GPa) will be due to the increase of bandwidth (or transfer integrals). The room temperature conductivity at 6.0 GPa was as high as 450 S cm^{-1}. The pressure dependence of the room temperature conductivity suggested a pressure-induced transition at around 5 GPa.

3.7. Magnetic Interactions in [Cu(dmdt)$_2$].

As previously mentioned, [$Cu(dmdt)_2$] exhibited Curie−Weiss behavior of $\chi = C/(T + \Theta)$ at high temperature (Θ = 180 K) and underwent an antiferromagnetic transition near 95 K (T_N). The Curie constant C of 0.375 emu/mol ($C = Ng^2\mu_B{}^2 s(s+1)/3k_B$, where s = 1/2 and N is the total number of $Cu(dmdt)_2$ molecules) implied that every crystallographically equivalent $Cu(dmdt)_2$ molecule possessed spin $^1/_2$. If the simple mean-field picture of a magnetic system composed of two sublattices with up (α) and down (β) spins can be applied, the effective field on α- and β-sites is known to be written as, $H_\alpha = -A_1M_\beta - A_2M_\alpha + H$ and $H_\beta = -A_1M_\alpha - A_2M_\beta + H$, where M_α (M_β) is the magnetic moment of the α-sublattice (β-sublattice), $-A_1M_\beta$ (A_2M_α) is the effective magnetic field on the α-sublattice produced by the β-sublattice (α-sublattice), and H is the external field.[26,27] If the magnetic interaction between the nth molecule with α spin and the surrounding jth molecule with β spin (ith molecule with α spin) is expressed as $-2J_{aj}s_ns_j$ ($-2J_{bi}s_ns_i$), A_1 and A_2 are given by the following equations, $A_1 = 4(\Sigma_jJ_{aj})/(Ng^2\mu_B{}^2)$ and $A_2 = 4(\Sigma_iJ_{bi})/(Ng^2\mu_B{}^2)$. Then, T_N and Θ are expressed as, $T_N = (C/2)(A_1 - A_2) = 2(\Sigma_jJ_{aj} - \Sigma_iJ_{bi})s(s+1)/3k_B$ and $\Theta = (C/2)(A_1 + A_2) = 2(\Sigma_jJ_{aj} + \Sigma_iJ_{bi})s(s+1)/3k_B$, where s = 1/2. Thus, $\Sigma_jJ_{aj} = (\Theta + T_N)/4 \approx 70k_B$ and $\Sigma_iJ_{bi} = (\Theta - T_N)/4 \approx 20k_B$, because T_N = 95 K and Θ = 180 K. It is well-known that the molecules i and j with intermolecular transfer integrals of t_{ij} interact antiferromagnetically with each other. The antiferromagnetic interaction ($-2J_{ij}s_is_j$) is roughly estimated as, $-2(t_{ij}{}^2/U)s_i \cdot s_j$, where U is on-site Coulomb energy and s are the spin operators. U for the $Cu(dmdt)_2$ molecule can be roughly estimated by assuming that one electron is located around the central C═C bond of the left dmdt ligand and the second electron is located around that of right ligand. Since the distance between these two C═C bonds is 12.3 Å, $U \approx 1.2$ eV. By adopting the extended Hückel approximation, t_{ij} can be estimated from the intermolecular overlap integrals (S_{ij}) of the SOMO of $Cu(dmdt)_2$: $t_{ij} = ES_{ij}$, where $E \approx -10$ eV.[28] As seen from Figure 6a, there are four different intermolecular overlap integrals between the central molecule (0th molecule) and the surrounding molecules (1−4th molecules). The overlap integrals calculated on the basis of the extended Hückel approximation were: $S_{01} = 6.1 \times 10^{-3}$, $S_{02} = 3.1 \times 10^{-3}$, $S_{03} = 1.5 \times 10^{-3}$, $S_{04} = 1.0 \times 10^{-3}$. The relatively large overlap integrals S_{01} and S_{02} suggest that molecules 0 and 1 and molecules 0 and 2 tend to be antiferromagnetically coupled to produce the plausible spin structure model shown in Figure 6a. If the antiferromagnetic coupling smaller than J_{02} can be neglected, $\Sigma_jJ_{aj} \approx 2(J_{01} + J_{02})$, where 2 denotes the number of equivalent intermolecular interactions. Using the estimated values of S_{01}, S_{02} and U, J_{01} and J_{02} were calculated as, 36 k_B and 9.3 k_B, respectively. Thus, $\Sigma_jJ_{aj} \approx 90$ k_B, which is larger than the value (70 k_B) derived from T_N (95 K) and Θ (180 K). However, considering the roughness of the assumptions used in these calculations, the agreement was quite satisfactory.

4. CONCLUSION

$[Cu(dmdt)_2]$ showed a large conductivity of 110 S cm^{-1} and weakly metallic behavior near room temperature. ESR experiments and susceptibility measurements showed Curie−Weiss behavior with a Weiss temperature of −180 K above 100 K. The Curie constant of 0.375 emu/mol showed that every $Cu(dmdt)_2$ molecule had a magnetic moment with $S = {}^1/_2$. These facts indicated that the conduction electrons and periodically arranged magnetic moments coexisted above 100 K. $[Cu(dmdt)_2]$ will suggest a cure to develop an unprecedented molecularly dense Kondo system. The rapid increase in resistivity slightly below 100 K and the abrupt decrease in ESR intensity near 95 K suggested that a coupled electric and magnetic transition took place near 95 K. The crystal structure studies performed down to 13 K revealed an extremely small thermal expansion coefficient for $[Cu(dmdt)_2]$ along the direction perpendicular to the layers of "dmdt dimers" with a "κ-type arrangement," connected to each other by Cu−S coordination bonds. To check the stability of the twisted conformation of the Cu-dithiolate complex, the conformational energies of individual $M(L)_2$ (M = Cu, Zn; L = dithiolate ligand) molecules were calculated with varying dihedral angles between the two dithiolate ligands. This revealed that the most stable dihedral angle of $Cu(L)_2$ was altered upon exchange of the ligand and/or change in oxidation state. The high-pressure four-probe resistivity measurements were performed using a DAC at 3.3−9.3 GPa. The insulating transition observed at 95 K and ambient pressure was almost suppressed even at the lowest pressure examined (3.3 GPa), except for an extremely small resistivity increase below 60 K ($R(1.9\text{ K})/R(60\text{ K}) \approx 1.6$ at 3.3 GPa). It is expected that the re-examination of the resistivity of the high quality $[Cu(dmdt)_2]$ crystal below 3 GPa will reveal the existence of the molecular conductor with three-dimensionally arranged magnetic moments embedded in a sea of π conduction electrons, and will provide a new frontier of magnetic molecular conducting systems. The antiferromagnetic interactions estimated from the intermolecular overlap integrals obtained by extended Hückel molecular orbital calculations revealed intermolecular magnetic interactions comparable to those derived from the experimentally obtained values of T_N and Θ.

■ ASSOCIATED CONTENT

Supporting Information

X-ray crystallographic files in CIF format. This material is available free of charge via the Internet at http://pubs.acs.org.

■ AUTHOR INFORMATION

Corresponding Author

*akoba@chs.nihon-u.ac.jp

Notes

The authors declare no competing financial interest.

■ ACKNOWLEDGMENTS

This study was financially supported by Grant-in-Aid on Innovative Areas (Nos. 20110002 and 20110003) and Grant-in-Aid for Scientific Research (Nos. 20350069 and 22224006) form the Ministry of Education, Culture, Sports, Science and Technology of Japan. The study was also supported by the "Ministry of Education, Culture, Sports, Science and Technology-Supported Program for the Strategic Research Foundation at Private Universities, 2009-2013 (No. S0901022)). We would like to thank Professor Nishibori of Nagoya University for very valuable information on the powder X-ray diffraction experiments on $[Cu(dmdt)_2]$, performed at the BL02B2 installed at the SPring-8 facility with the approval of the Japan Synchrotron Radiation Research Institute (JASRI).

■ REFERENCES

(1) Tanaka, H.; Okano, Y.; Kobayashi, H.; Suzuki, W.; Kobayashi, A. *Science* **2001**, *291*, 285−287.

(2) Kobayashi, A.; Tanaka, H.; Kobayashi, H. *J. Mater. Chem.* **2001**, *11*, 2078−2088.

(3) Kobayashi, A.; Fujiwara, E.; Kobayashi, H. *Chem. Rev.* **2004**, *104*, 5243−5264.

(4) Suzuki, W.; Fujiwara, E.; Kobayashi, A.; Fujishiro, Y.; Nishibori, E.; Takata, M.; Sakata, M.; Fujiwara, H.; Kobayashi, H. *J. Am. Chem. Soc.* **2003**, *125*, 1486−1487. (b) Zhou, B.; Shimamura, M.; Fujiwara, E.; Kobayashi, A.; Higashi, T.; Nishibori, E.; Sakata, M.; Cui, H.; Takahashi, K.; Kobayashi, H. *J. Am. Chem. Soc.* **2006**, *128*, 3872−3873.

(5) Seo, H.; Ishibashi, S.; Okano, Y.; Kobayashi, H.; Kobayashi, A.; Fukuyama, H.; Terakura, K. *J. Phys. Soc. Jpn.* **2008**, *77*, 023714.

(6) Hara, Y.; Miyagawa, K.; Kanoda, K.; Shimamura, M.; Zhou, B.; Kobayashi, A.; Kobayashi, H. *J. Phys. Soc. Jpn.* **2008**, *77*, 053706.

(7) Ishibashi, S.; Tanaka, H.; Kohyama, M.; Tokumoto, M.; Kobayashi, A.; Kobayashi, H.; Terakura, K. *J. Phys. Soc. Jpn.* **2005**, *74*, 843−846.

(8) Zhou, B.; Yajima, H.; Kobayashi, A.; Okano, Y.; Tanaka, H.; Kumashiro, T.; Nishibori, E.; Sawa, H.; Kobayashi, H. *Inorg. Chem.* **2010**, *49*, 6740−6747.

(9) Tanaka, H.; Kobayashi, H.; Kobayashi, A. *J. Am. Chem. Soc.* **2002**, *124*, 10002−10003.

(10) Ishibashi, S.; Terakura, K.; Kobayashi, A. *J. Phys. Soc. Jpn.* **2008**, *77*, 024702.

(11) Binet, L.; Fabre, J. M.; Montginoul, C.; Simonsen, K. B.; Becher, J. *J. Chem. Soc., Perkin Trans. 1* **1996**, 783−788. (b) Binet, L.; Montginoul, C.; Fabre, J. M.; Ouahab, L.; Golhen, S.; Becher, J. *Synth. Met.* **1997**, *86*, 1825−1826. (c) Fujiwara, E.; Kobayashi, A.; Fujiwara, H.; Kobayashi, H. *Inorg. Chem.* **2004**, *43*, 1122−1129.

(12) *CrystalStructure 3.8.0*; Crystal Structure Analysis Package; Rigaku and Rigaku/MSC: The Woodlands, TX, 2000−2006.

(13) Delley, B. *J. Chem. Phys.* **1990**, *92*, 508−517. (b) Delley, B. *J. Chem. Phys.* **2000**, *113*, 7756−7764 ; $DMol^3$ is available as part of Material Studio.

(14) Perdew, J. P.; Burke, K.; Ernzerhof, M. *Phys. Rev. Lett.* **1996**, *77*, 3865−3868.

(15) Adachi, T.; Tanaka, H.; Kobayashi, H.; Miyazaki, T. *Rev. Sci. Instrum.* **2001**, *72*, 2358−2360. (b) Kobayashi, A.; Tanaka, H.; Kumasaki, M.; Torii, H.; Narymbetov, B.; Adachi, T. *J. Am. Chem. Soc.* **1999**, *121*, 10763−10771.

(16) Cui, H.; Brooks, J. S.; Kobayashi, A.; Kobayashi, H. *J. Am. Chem. Soc.* **2009**, *131*, 6358−6359.

(17) Aumuller, A.; Erk, P.; Klebe, G.; Hunig, S.; von Schutz, J. U.; Werner, H.-P. *Angew. Chem.* **1986**, 759−761. (b) Hunig, S.; Herberth, E. *Chem. Rev.* **2004**, *104*, 5535−5563.

(18) Kobayashi, A.; Kato, R.; Kobayashi, H.; Mori, T.; Inokuchi, H. *Solid State Commun.* **1987**, *64*, 45−51. (b) Kato, R.; Kobayashi, H.; Kobayashi, A. *J. Am. Chem. Soc.* **1989**, *111*, 5224−5232. (c) Kato, R. *Bull. Chem. Soc. Jpn.* **2000**, *73*, 515−534.

(19) Coronado, E.; Day, P. *Chem. Rev.* **2004**, *104*, 5419−5448.

(20) Kobayashi, H.; Cui, H.; Kobayashi, A. *Chem. Rev.* **2004**, *104*, 5265−5288.

(21) Idobata, Y.; Zhou, B.; Kobayashi, A; Kobayashi, H. *J. Am. Chem. Soc.* **2012**, *134*, 871−874.

(22) Kobayashi, A.; Kato, R.; Kobayashi, H.; Moriyama, S.; Nishio, Y.; Kajita, K.; Sasaki, W. *Chem. Lett.* **1987**, 459−462. (b) Kobayashi, H.; Kobayashi, A.; Tajima, H. *Chem. Asian J.* **2011**, *6*, 1688−1704.

(23) Zhou, B.; Kobayashi, A.; Okano, Y.; Cui, H.; Graf, D.; Brooks, J. S.; Nakashima, T.; Aoyagi, S.; Nishibori, E.; Sakata, M.; Kobayashi, H. *Inorg. Chem.* **2009**, *48*, 10151−10157.

(24) Yamamoto, K.; Fujiwara, E.; Kobayashi, A.; Fujishiro, Y.; Nishibori, E.; Sakata, M.; Takata, M.; Tanaka, H.; Okano, Y.; Kobayashi, H. *Chem. Lett.* **2005**, *34*, 1090−1091.
(25) Matsubayashi, G.; Takahashi, K.; Tanaka, T. *J. Chem. Soc., Dalton Trans.* **1988**, 967−972.
(26) Kittel, C. *Introduction to Solid State Physics*; John Wiley & Sons: New York, 1996.
(27) Adachi, K. *Magnetism of Compounds (in Japanese)*; Shokabo: Tokyo, 1996.
(28) Mori, T.; Katsuhara, M. *J. Phys. Soc. Jpn.* **2002**, *71*, 826−844.